



Cite this: *RSC Adv.*, 2021, **11**, 30781

The recent development of donepezil structure-based hybrids as potential multifunctional anti-Alzheimer's agents: highlights from 2010 to 2020

Rzgar Tawfeeq Kareem,^a Fahimeh Abedinifar,^b Evan Abdolkareem Mahmood,^c Abdol Ghaffar Ebadi,^d Fatemeh Rajabi^{b*}^e and Esmail Vessally^b^e

Dementia is a term used to define different brain disorders that affect memory, thinking, behavior, and emotion. Alzheimer's disease (AD) is the second cause of dementia that is generated by the death of cholinergic neurons (especially acetylcholine (ACh)), which have a vital role in cognition. Acetylcholinesterase inhibitors (AChEIs) affect acetylcholine levels in the brain and are broadly used to treat Alzheimer's. Donepezil, rivastigmine, and galantamine, which are FDA-approved drugs for AD, are cholinesterase inhibitors. In addition, scientists are attempting to develop hybrid molecules and multi-target-directed ligands (MTDLs) that can simultaneously modulate multiple biological targets. This review highlights recent examples of MTDLs and fragment-based strategy in the rational design of new potential AD medications from 2010 onwards.

Received 12th May 2021

Accepted 14th August 2021

DOI: 10.1039/d1ra03718h

rsc.li/rsc-advances

1. Introduction

Alzheimer's disease (AD) is a progressive, chronic, and incurable neurological disorder that affects millions of people worldwide. According to the World Alzheimer report, there are currently more than 30 million people with Alzheimer's disease, with estimates that this number will increase up to 115 million in 2050.¹ The symptoms of this disease consist of memory loss, challenges in planning or solving problems, changes in mood and personality, and decreased judgment or decision-making abilities.² Cholinergic neuron death, diminishing

^aDepartment of Chemistry, College of Science, University of Bu Ali Sina, Hamadan, Iran

^bSchool of Chemistry, College of Science, University of Tehran, Tehran, Iran

^cCollege of Health Sciences, University of Human Development, Sulaimaniyah, Kurdistan region of Iraq

^dDepartment of Agriculture, Jouybar Branch, Islamic Azad University, Jouybar, Iran

^eDepartment of Chemistry, Payame Noor University, P.O. Box 19395-3697, Tehran, Iran. E-mail: f_rajabi@pnu.ac.ir



Rzgar Tawfeeq Kareem was born in Sulaimaniyah, Iraq, in 1988. He received his B.S. degree in pure chemistry from Garmian University, Iraq, and his M.S. degree in analytical chemistry from the University of Siirt, Turkey. Now, he is completing his PhD degree at the University of Bu Ali Sina.

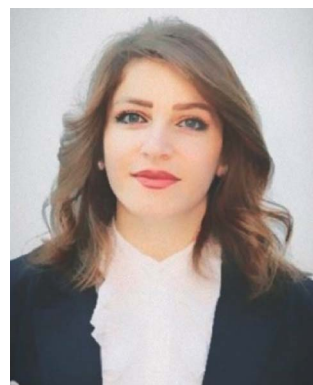


Fahimeh Abedinifar was born in 1983 in Qazvin, Iran. She received her M.Sc. in organic chemistry from IKIU University in 2009 under the guidance of Prof. M. Alavi. She carried out her PhD degree under the supervision of Dr M. Farnia at Tehran university in 2018. She collaborated as a postdoctoral researcher with Dr Larijani's research team at the Institute of Endocrinology and Metabolism Clinical Sciences, Tehran University of Medical Sciences, Iran, from 2019 to 2020. Her research interests include the synthesis of biologically active heterocycles and application of new catalysts in multicomponent reactions.



neurotransmitter acetylcholine (ACh) levels in the brain,³ metal dyshomeostasis, oxidative stress,⁴ deficiency in steroid hormones, higher inflammatory mediators, deposition of β -amyloid (A β),⁵ and tau-protein⁶ have been mentioned as the main causes of AD.

Since this disease has a multifactorial nature, there is no effective treatment. Multi-target-directed ligands (MTDLs) are single molecules that can simultaneously modulate multiple



Evan Abdolkareem Mahmood was born in Erbil, Kurdistan Region, Iraq, in 1990. She is a Biochemistry lecturer. She lives in Iraq/Kurdistan Region. About her educational background, she got a Bachelor degree of Chemistry from University of Sulaimaniyah, College of Science. She completed her Master Degree in Biochemistry at Yüzüncü Yil University at Van city, Turkey.

She is an Assistant Lecturer at University of Human Development, College of Health Science. Also, she worked as a Head of Pharmacy department at National Institute in Sulaimaniyah/Iraq. Her research interests include health, environment, chemistry, clinical biochemistry science.

targets in neurodegenerative disorders. Multi-target-directed ligands (MTDLs) generally are designed by connecting the pharmacophores of target ligands and are produced by chemical syntheses. Degeneration in the basal forebrain leads to a deficiency in central cholinergic transmission, which is believed to be a significant neurochemical and pathological characteristic of AD.⁷ The cholinergic hypothesis is one of the oldest hypotheses that takes the role of ACh role into account in



Dr Fatemeh Rajabi was born in Qazvin, Iran. She received her doctoral degree in organic chemistry at the Sharif University of Technology in 2005. In 2004, she received a British Council Scholarship and joined Prof. James Clark research group at the University of York (UK) in the Green Chemistry Centre of Excellence where the group works at the frontiers of modern chemical research in the areas of clean synthesis, catalysis, novel materials and application of renewable resources. She has become a faculty member at the Payame Noor University since 2006. In 2010 and 2017, she received DAAD Research Stays for University Academics and Scientists and joined Prof. Werner Thiel research group at the Technische Universität Kaiserslautern, Germany, where they work on the synthesis and characterization of homogeneous and heterogeneous (photo)catalysts and the elucidation of reaction mechanisms and structure/activity relationships. In 2012–2013, 2014, and 2018 she received a prestigious Alexander Von Humboldt Fellowship and was re-invited to join Prof. Werner Thiel research group and establish long collaboration. Her main research interests is the synthesis of hybrid organic-inorganic mesoporous silica-based organometallic complexes applied to green and sustainable catalysis.



Dr Abdol Ghaffar Ebadi finished his doctoral degree in Environmental Biotechnology (Algology) from Tajik Academy of Sciences. Now he is a researcher in TAS in Tajikistan and faculty member at the Islamic Azad University of Jouybar in Mazandaran. Dr Ebadi published more than 400 scientific papers in qualified international journals and attended more than 50 international conferences. He has

cooperation with many research project teams around world such as China, Malaysia, and Thailand. His interests are Environmental Biotechnology, Biochemistry, Gene pathways in the phytoremediation processes.



Esmail Vessally was born in Sharabiyan, Sarab, Iran, in 1973. He received his B.S. degree in pure chemistry from university of Tabriz, Tabriz, Iran, and his M.S. degree in organic chemistry from Tehran university, Tehran, Iran, in 1999 under the supervision of Prof. H. Pir-Elahi. He completed his PhD degree in 2005 under the supervision of Prof. M. Z. Kassaei. Now he is working at Payame Noor University as Professor in organic chemistry. His research interests include theoretical organic chemistry, new methodologies in organic synthesis and spectral studies of organic compounds.



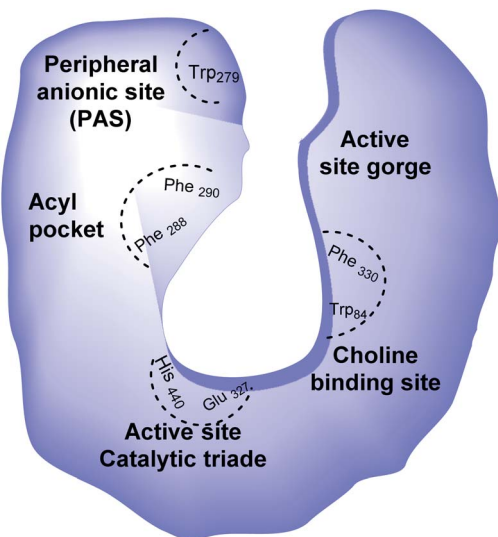


Fig. 1 Schematic representation of AChE binding sites; His: histidine, Glu: glutamate, Phe: phenylalanine, Trp: tryptophan.

animal and human behavior. Even though the cholinergic hypothesis is the most developed, the other hypothesis, A β peptide aggregation, describes how this aggregation could affect the AChE enzyme and is considered the most important. Hydrolysis of acetylcholine in the brain occurs by two types of cholinesterases (ChE): acetylcholinesterase enzyme (AChE) and butyrylcholinesterase (BuChE). Acetylcholinesterase enzyme (AChE) possesses two main binding sites for drug interaction, the catalytic site and the peripheral anionic site (PAS) (Fig. 1).⁸

In the amyloid aggregation process, the AChE anionic binding site is believed to be of paramount importance. Hence,

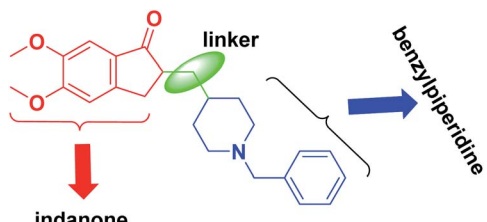


Fig. 2 Structure of donepezil.

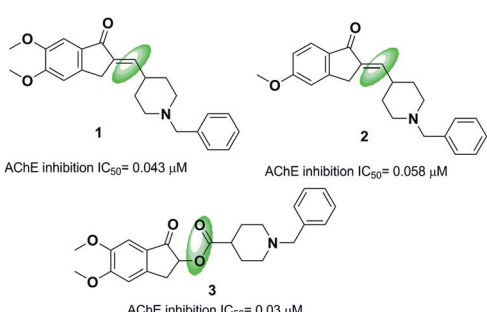
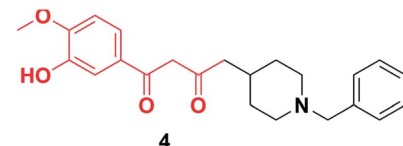
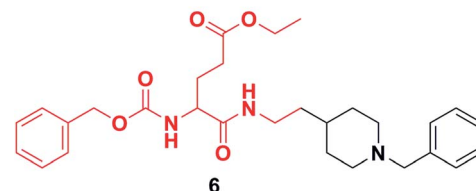
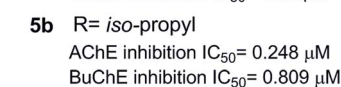
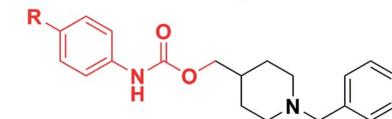


Fig. 3 Donepezil analogs with different linkers.



AChE inhibition $IC_{50} = 0.187 \mu M$
 BuChE inhibition $IC_{50} = 12.4 \mu M$



AChE inhibition $IC_{50} = 4.99 \mu M$
 BuChE inhibition $IC_{50} = 0.4 \mu M$

Fig. 4 Donepezil analogs with aromatic molecules.

this site is targeted as an alternative site by AChE inhibitors, which function as multi-target ligands that cause a decrease in the formation of senile plaque. Therefore, cholinomimetic therapy with anticholinergic drugs is the main approach in treating AD. The acetylcholinesterase inhibitor (AChEI) increases endogenous AChE levels and enhances cholinergic neurotransmission in the brain. Among the investigated acetylcholinesterase inhibitors, donepezil (2-((1-benzylpiperidin-4-yl)methyl)-5,6-dimethoxy-2,3-dihydro-1H-inden-1-one) is of most highly effective and well-known FDA-approved drug (Fig. 2).⁹ Donepezil consists of dimethoxy indanone, which is connected to N-benzylpiperidine via a methylene linker.

A molecular docking investigation of donepezil showed that the indanone moiety fuses with the PAS of AChE, and the benzylic part links with the catalytic anionic site (CAS).¹⁰ The N-

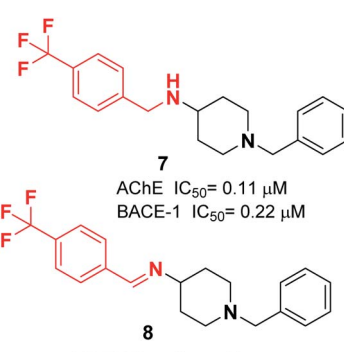


Fig. 5 Structure of donepezil-based benzylamine derivatives.

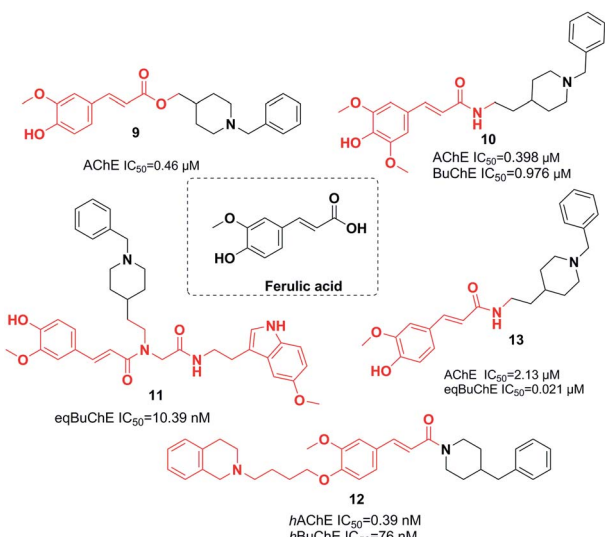


Fig. 6 Structure of most potent donepezil–ferulic acid hybrids.

benzylpiperidine group is situated onto the narrowest active-site cavity section. It interacts with four amino acid residues, Tyr-70, Asp-72, Tyr-121, and Tyr-334, in the anionic site.¹¹ A large number of reviews have been published on Alzheimer's topics.^{12,13} Still, this review summarizes recent findings in AD research by emphasizing simple synthetic compounds with modified donepezil structures that act as MTDLs. We focused on the current literature and produced a collection of all hybrids of *N*-saturated heterocyclic compounds based on the structure of donepezil that were published from 2010 until now. We categorized this review into main sections of donepezil derivatives with different linkers for ease of reading, replacing indanone with heterocycles, and inserting piperazine/pyrrolidine instead of piperidine to produce donepezil-like structures. This current review will provide insights into the design and development of novel therapeutics for treating AD.

2. Donepezil-like derivatives with different linkers

One strategy in designing new acetylcholinesterase inhibitors (AChEI) is to create different linkers in the donepezil structure. Costanzo *et al.* synthesized indanonylidene precursors of donepezil through condensing the indanone nucleus and derivatives of *N*-benzylpiperidine-4-carboxaldehyde in the presence of a basic resin, Amberlyst A-26. The biological assessment indicated that compounds 1 and 2 demonstrated higher dual activity and decreased values of IC₅₀ toward the AChE enzyme and BACE-1 enzyme as compared to donepezil (Fig. 3).¹⁴ Greunen *et al.* synthesized two libraries of possible AChE inhibitors according to the AChE molecular skeleton by replacing the piperidine ring with *N*-saturated ring systems in different sizes and introducing various linker piperidine rings to the indanone in donepezil. Replacement of a methyl linker with an ester moiety resulted in a complete loss of activity in all but one case, where 5,6-dimethoxy-1-oxo-2,3-dihydro-1*H*-inden-2-yl-1-benzylpiperidine-4-carboxylate 3 yielded 0.03 μM IC₅₀ towards AChE *in vitro* (Fig. 3).¹⁵

3. Donepezil-like derivatives with the replacement of the indanone part

As mentioned in the introduction, donepezil consists of an indanone moiety. Replacement of this part with various compounds has led to new hybrids of donepezil with various inhibitory activities.

3.1. Replacement of indanone with aromatics

Yan *et al.* produced a new series of derivatives by fusing donepezil and curcumin pharmacophores under aldol condensation.¹⁶ They investigated the AChE inhibitor activity, Aβ-aggregation, metal chelation, and antioxidant activities. Among the synthetic targets, compound 4 showed the highest

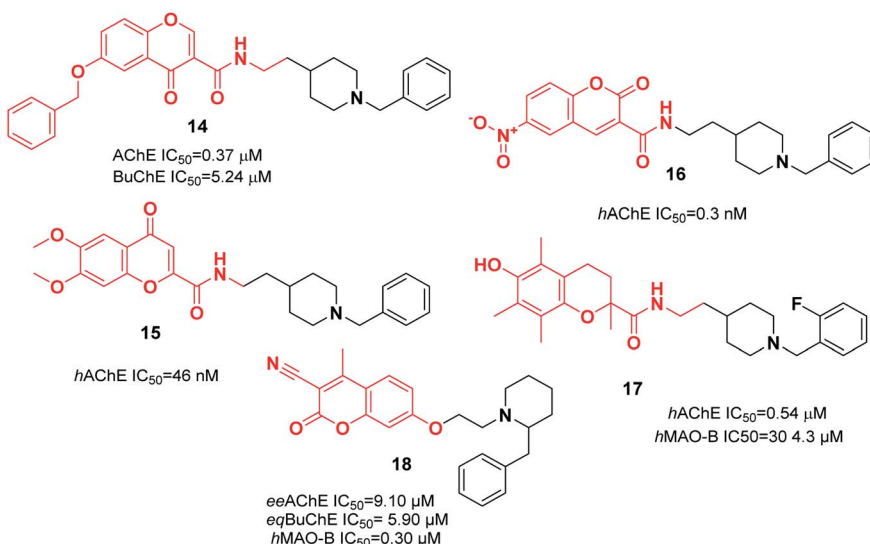


Fig. 7 Donepezil–flavonoid hybrids.



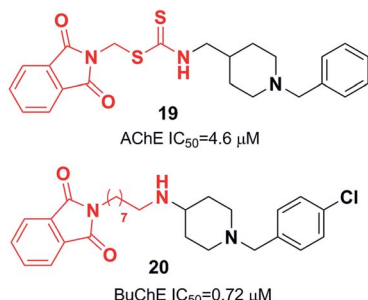


Fig. 8 Structure of phthalimide-dithiocarbamate hybrids.

selectivity ratio of 66.3 for BuChE/AChE, which was considerably better than the reference tacrine and galantamine with a selectivity ratio of 0.15 and 25.3 and slightly worse than donepezil with a selectivity ratio of 85.4. Compound 4 also demonstrated potent inhibition of self-induced $\text{A}\beta$ aggregation (Fig. 4). Košák *et al.* developed a class of *N*-benzylpiperidine carbamates as viable anti-Alzheimer agents. Compound 5a showed selective *h*BuChE and *h*MAO-B inhibitor activity (with an IC_{50} of 0.178 μM), but 5b exhibited selective *h*AChE inhibition (Fig. 4).¹⁷ In 2017, Monjas prepared L- and D-glutamic acid derivatives with the *N*-benzylpiperidine fragment in the γ -position in the presence of *Mucor miehei* and *Candida antarctica* lipases in high yield. The multifunctional profile of synthesized compound 6 exhibited stronger inhibition of human ChE activity (Fig. 4).¹⁸

At ambient temperature, the treatment of 1-benzylpiperidin-4-amine with disparate aromatic aldehydes under glacial acetic acid in absolute ethanol generated imine hybrids. The reduction of imines in NaBH_4 produced benzylamine derivatives in good yield (Fig. 5). These two series of amine derivatives were assessed as multi-functional AChE and BACE-1 inhibitors having moderate to excellent activities. Compared with donepezil, which exhibited 42.1-fold AChE selectivity (with an IC_{50} of 0.44 μM for AChE, and IC_{50} of 0.28 μM for BACE-1), the selective inhibition of compound 7 was 28.2-fold for AChE, and it displayed self-induced as well as AChE-induced $\text{A}\beta$ aggregation inhibition in the thioflavin T-assay. Docking studies revealed that 7 and 8 elicited similar interactions at the PAS, except for additional π - π stacking and π -cation interactions with the Tyr341 residue. The benzyl portion of the compounds exhibited

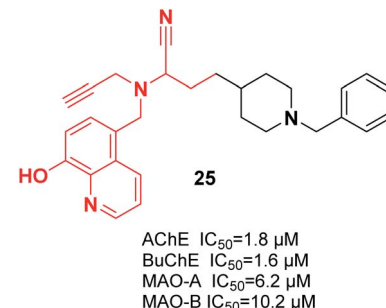


Fig. 10 Structure of a donepezil-8-hydroxyquinoline derivative as a mixed-type AChE inhibitor.

interactions with Trp86 (π - π stacking or π -cation) and Glu202 (electrostatic) residues at anionic subsites (Fig. 5).¹⁹

3.2. Replacement of indanone with ferulic acid derivatives

Ferulic acid, which is found in plant cell walls, is a hydroxycinnamic acid with pharmacological activities.²⁰ In a study carried out by Dias *et al.*, the synthesis, design, and pharmacological assessment of novel molecular hybrids of feruloyl-donepezil were reported. The *N*-benzylpiperidine pharmacophore of donepezil is responsible for its sufficient recognition through AChE and the subunit feruloyl, which exists in curcumin and ferulic acid. Based on the *in vitro* results, all the compounds mentioned demonstrated potent AChE inhibitory activity, moderate antioxidant properties, neuroprotection of neuronal cells against the oxidative process, and significant metal chelation of Fe^{2+} and Cu^{2+} . Compound 9 had the greatest AChE inhibitor potency (Fig. 6).²¹

In 2016, the design and synthesis of other donepezil-ferulic acid hybrids were carried out. The synthetic molecules were assessed as MTDLs against AD. An *in vitro* assay demonstrated that there was moderate AChE and BuChE inhibition by compound 10. This compound exhibited considerable antioxidant activity (1.78 Trolox equivalents through the ABTS method, with an IC_{50} of 24.9 μM through the DPPH method) (Fig. 6).²² Benchekroun *et al.* prepared donepezil-ferulic acid hybrids (DFAHs) through one-pot Ugi-4CR in low to moderate yield. They found that hybrid (*E*)-*N*-(2-(1-benzylpiperidin-4-yl)ethyl)-3-(4-hydroxy-3-methoxyphenyl)-*N*-(2-((2-(5-methoxy-1*H*-indol-3-yl)ethyl)amino)-2-oxoethyl)acrylamide 11 was a selective *eq*BuChE, and the oxygen radical-absorbing capacity of this compound was 8.71 μmol (Fig. 6).²³

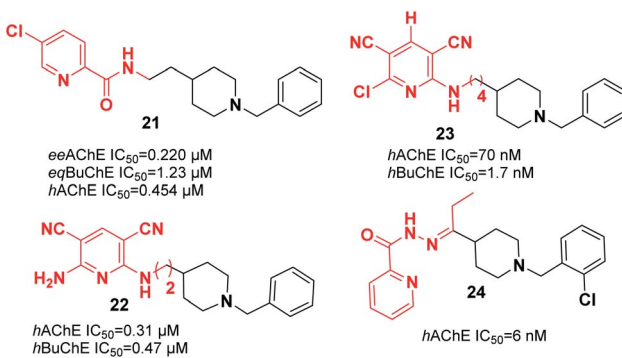


Fig. 9 Pyridine-donepezil hybrids with ChEi activity.

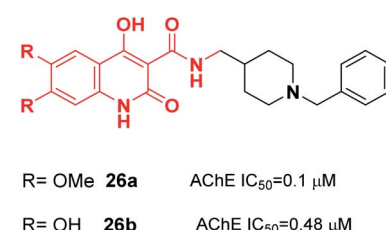


Fig. 11 Structure of a quinolone-benzylpiperidine derivative as a new acetylcholinesterase inhibitor.

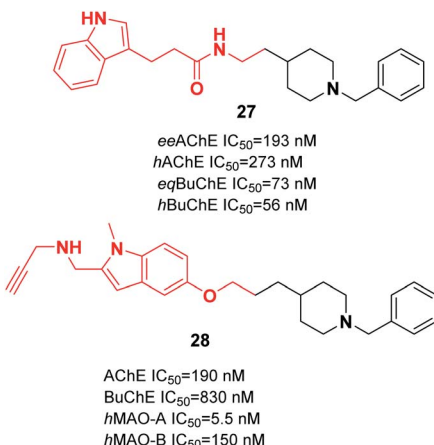


Fig. 12 Multitarget molecules based on donepezil–indole hybrids.

Sang *et al.* synthesized new derivatives of ferulic acid-*O*-alkylamine and then evaluated them against AD. Based on *in vitro* studies, all exhibited considerable inhibitory activity toward BuChE, acceptable self-induced aggregation ($A\beta$), and functioned as viable antioxidants. Specifically, compound **12** was a satisfactory AChE inhibitor with the greatest BuChE inhibition potency. It exhibited an inhibitory impact upon self-induced aggregation of $A\beta_{1-42}$ (50.8%) and self-induced aggregation of $A\beta_{1-42}$ (38.7%), moderate antioxidant activity with 0.55 eq. of Trolox, acceptable protection against H_2O_2 -induced PC12 cell injury, and low toxicity (Fig. 6).²² Estrada *et al.* linked cinnamic-related structures to *N*-benzylpiperidine. Compound **13** in series demonstrated moderate inhibition of *hAChE* with an IC_{50} of 0.39 and inhibition of *hBuChE* with an IC_{50} of 76 nM. The existence of the *p*-hydroxy group was necessary for inhibition of the cinnamic fragment (Fig. 6).²⁴

3.3. Donepezil-like derivatives with replacement of indanone with heterocycles

3.3.1. Replacement of indanone with oxygen-containing heterocycles. The chromone structure, 4*H*-1-benzopyran-4-one, has been considered the pharmacophore of many active compounds in flavones and isoflavones. All of these structures are considered scaffolds that can be used to develop *hMAO* inhibitors. Combining the benzylpiperidine moieties of donepezil and

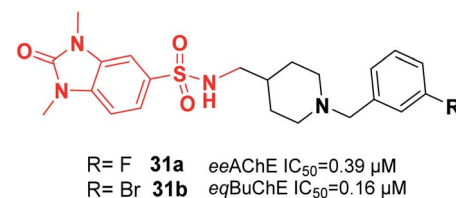


Fig. 14 Structure of a dimethylbenzimidazolinone–benzylpiperidine hybrid.

chromone resulted in the new dual inhibitors AChE and MAO-B. Among the synthetic targets, compound **14** exhibited the most proportionate probability of inhibiting ChEs and greatest *hMAO-B* selectivity ($IC_{50} = 0.272 \mu$ M and SI of 247, respectively). Also, kinetic and molecular modeling indicated that compound **14** is a mixed type of inhibitor that simultaneously binds to the PAS and CAS of AChE and penetrates the blood–brain barrier (BBB). In addition, it exhibits low toxicity against rat pheochromocytoma (PC12) cells (Fig. 7).²⁵ In 2018, Estrada *et al.* explored neurogenic and neuroprotective donepezil–flavonoid hybrids (DFHs). These targets showed affinities toward the sigma-1 receptor (σ -1R), and inhibition of AChE, monoamine oxidases (MAOs), and 5-lipoxygenase (5-LOX). The most potent ligand was *N*-(2-(1-benzylpiperidin-4-yl)ethyl)-6,7-dimethoxy-4-oxo-4*H*-chromene-2-carboxamide **15**, which demonstrated a moderate 5-LOX inhibition with an IC_{50} of 74.3 μ M and acceptable *hAChE* inhibition with an IC_{50} of 46 nM (Fig. 7).²⁶

In a research study performed by Asadipour *et al.*, derivatives of coumarin-3-carboxamide were synthesized that were connected to *N*-benzylpiperidine. Based on the results, almost all the compounds exerted potent activity against AChE in the nM concentration range. Among them, compound **16**, with a *N*-methyl carboxamide linker and 6-nitro substituent, demonstrated the most potent activity and the highest selectivity of 26 300 with 46-fold more potency than the standard drug donepezil against AChE (Fig. 7).²⁷ To synthesize multifunctional anti-AD agents, donepezil and Trolox pharmacophores were fused into one molecule by Cai *et al.* Among the targets, *N*-(2-(1-(2-fluorobenzyl)piperidin-4-yl)ethyl)-6-hydroxy-2,5,7,8-tetramethylchromane-2-carboxamide **17** exhibited balanced functions with an acceptable inhibitory effect upon *hAChE* and *hMAO-B*, considerable antioxidant activity with an IC_{50} of 41.33 μ M, outstanding copper chelation, $A\beta_{1-42}$ aggregation inhibition impact, and less hepatotoxicity toward cell lines HePG2,

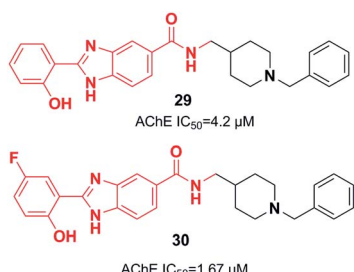


Fig. 13 Hydroxy benzimidazole–donepezil hybrids that are multi-target-directed ligands.

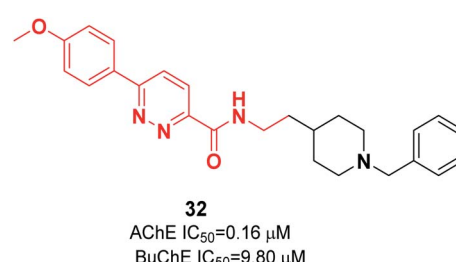


Fig. 15 Structure of a phenylpyridazine-3-carboxamide-benzylpiperidine hybrid.



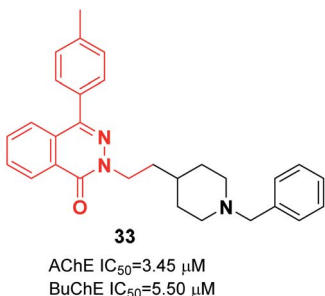


Fig. 16 Structure of a phthalazin-1(2H)-one-donepezil hybrid.

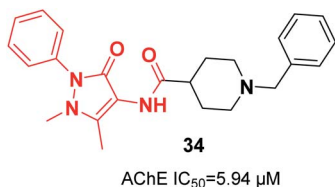


Fig. 17 Structure of a pyrazole-benzylpiperidine derivative.

PC12, and BV-2 (Fig. 7).²⁸ The design and synthesis of 7-substituted coumarin derivatives were carried out by Joubert *et al.* These compounds retained the *N*-benzylpiperidine function of donepezil (ChE inhibitor) and the coumarin structure (MAO-B inhibitor) connected at the 7-position by an alkyl ether linkage. According to the biological assay results, compound 18 had the highest multifunctional agent potency, and exhibited a satisfactory *ee*AChE inhibition and potent selective *h*MAO-B inhibition ($SI > 33$). According to the molecular modeling, compound 18 simultaneously binds to the PAS, mid-gorge, and CAS of AChE and BuChE (Fig. 7).²⁹

3.3.2. Replacement of indanone with nitrogen-containing heterocycles. The design and synthesis of phthalimide-dithiocarbamate hybrids were performed by Asadi *et al.* based on the donepezil pharmacophore. All lead compounds demonstrated cholinesterase inhibitory activity, and a benzylpiperidine derivative with methylene linker 19 had the greatest inhibitory impact with an IC_{50} of $4.6 \mu\text{M}$. There was 2.5-fold greater activity of this compound as compared to rivastigmine ($\text{IC}_{50} = 11.07 \mu\text{M}$) (Fig. 8).³⁰ Więckowska *et al.* provided donepezil derivatives with an *N*-benzylpiperidine moiety mixed with indole or phthalimide moieties connected by an alkyl linker for mixing anticholinesterase and β -amyloid anti-aggregation activities in one molecule. Among the 28 targets, (2-(8-(1-(3-chlorobenzyl)

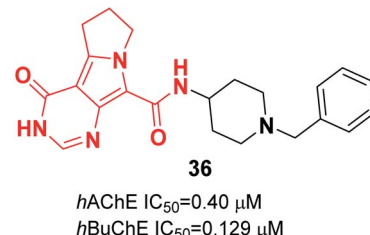


Fig. 19 Structure of a pyrrolizine-benzylpiperidine hybrid.

piperidin-4-yl amino)octyl)isoindoline-1,3-dione) 20 was a BuChE inhibitor with an IC_{50} of $0.72 \mu\text{M}$, and it exhibited β -amyloid anti-aggregation activity with inhibition of 72.5% at $10 \mu\text{M}$. It penetrates the BBB (Fig. 8).³¹

Substituting the indanone fragment of donepezil with the benzamide or 2-picolinamide moiety introduced a novel MTDL that exhibited potent inhibitory activities towards MAO-A, MAO-B, and AChE. Compound 21, *N*-(2-(1-benzylpiperidin-4-yl)ethyl)-5-chloropicolinamide, was the most potent agent with moderate cholinesterase inhibition activity in comparison with galanthamine as a reference (Fig. 9). It showed satisfactory inhibitory activity toward MAO-B with an IC_{50} of $3.14 \mu\text{M}$ and IC_{50} of $13.4 \mu\text{M}$ for MAO-A. Also, 21 can be considered a metal chelator, and it has the ability to cross the BBB with a low level of toxicity to PC12 cells.³²

Samadi *et al.* attached the *N*-benzylpiperidine moiety of donepezil to 2-aminopyridine derivatives and synthesized a novel series of considerably potent donepezil-aminopyridine hybrids. The most potent *h*AChE inhibitor was 2-amino-6-((3-(1-benzylpiperidin-4-yl)propyl)amino)pyridine-3,5-dicarbonitrile pyridonepezil 22, and its activity was 2.6-fold less compared to donepezil for *h*BuChE (IC_{50} (*h*AChE) = 9.4 nM ; IC_{50} (*h*BuChE) = $6.6 \mu\text{M}$) (Fig. 9).³³ In 2013, Samadi *et al.* developed 6-chloropyridonepezils and evaluated them against *h*AChE and *h*BuChE.³⁴ According to the biological evaluation, the novel compounds are inhibitors of cholinesterase in the sub-micromolar range. Particularly, 6-chloro-pyridonepezil 23 was the most potent target, being 625-fold more selective for *h*AChE than *h*BuChE. It can be considered a selective dual AChEI for further pharmacological developments in AD treatment (Fig. 9). Novel molecules were produced through the interaction of the *N*-benzylpiperidine moiety of donepezil with pyridine hydrazide, which exhibited greater AChE inhibition and showed higher selectivity over BuChE. For the most active compound 24, the IC_{50} was 6 nM with the capability to chelate cupric ion (Fig. 9).³⁵

It was reported that a new hybrid of donepezil-8-hydroxyquinoline was a multifunctional molecule that can be used to treat AD. Among the molecules, racemic α -aminonitrile-4-(1-benzylpiperidin-4-yl)-2-((8-hydroxyquinolin-5-yl)methyl)(prop-2-yn-1-yl)amino)butane nitrile 25 was the most promising compound and exhibited mixed-type AChE inhibitory effects and metal-chelating characteristics (Fig. 10).³⁶

Donepezil-quinolone carboxamide analogs were synthesized by Pudlo *et al.* Derivative 26a with the methoxy group and 26b

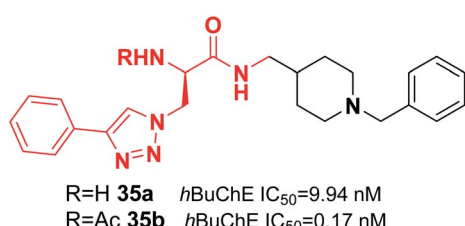


Fig. 18 Structure of an azido 1,2,3-triazoles-benzylpiperidine analog as a selective BuChE inhibitor.



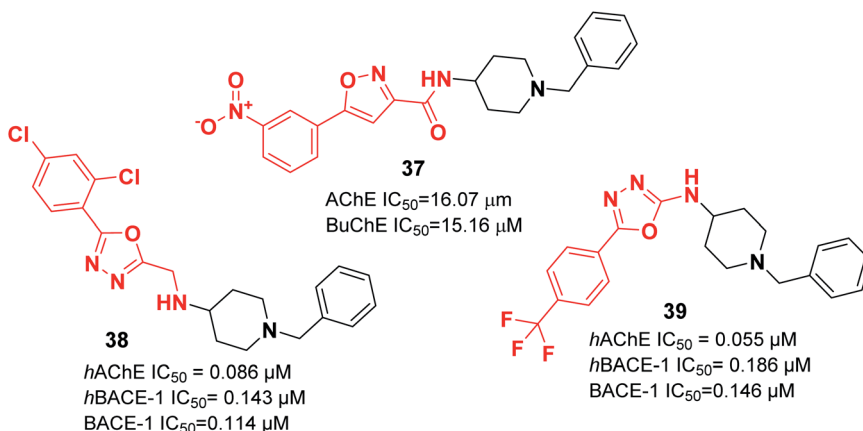


Fig. 20 Structure of isoxazole/oxadiazole-benzylpiperidine hybrids.

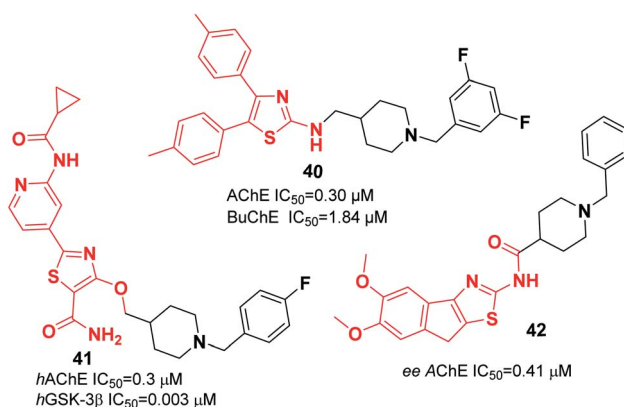


Fig. 21 Structure of thiazole-benzylpiperidine scaffolds.

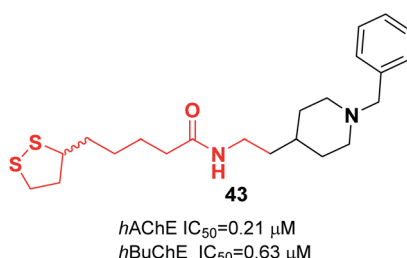


Fig. 22 A lipoic acid-based benzylpiperidine hybrid.

with the hydroxy group were potent and highly selective AChE inhibitors (Fig. 11).³⁷

Wang *et al.* produced novel *N*-benzylpiperidine-indole hybrids with a carboxamide linker. Compound 27 with a two-carbon spacer exhibited satisfactory AChE and BuChE inhibition, with an average inhibition (56.3%) of Aβ aggregation at 20 μM, and satisfactory antioxidant activity (3.28 Trolox equivalent by ORAC assay). Moreover, 27 chelated metal ions, decreased the death of PC12 cells caused by oxidative stress, and was able to cross the BBB. The molecular docking of 27 represents a mixed-type inhibitor that simultaneously binds with the CAS and PAS of AChE (Fig. 12).³⁸ Based on the benzylpiperidine

portion of donepezil and the indole derivative of propargylamine, various multi-target molecules were synthesized by Bautista-Aguilera *et al.* Among the synthetic compounds, *N*-(5-(3-(1-benzylpiperidin-4-yl)propoxy)-1-methyl-1*H*-indol-2-yl) methylprop-2-yn-1-amine 28 was the most potent inhibitor (Fig. 12).³⁹

Piemontese *et al.* conjugated the benzylpiperidine part of donepezil with the benzimidazole bioactive molecule. The biological assessment showed that new targets have potential anti-Aβ aggregation capacity, antioxidant activity, and metal-chelating properties. The synthetic lead 29 showed satisfactory AChE inhibition activity and moderate inhibition of Aβ₁₋₄₂

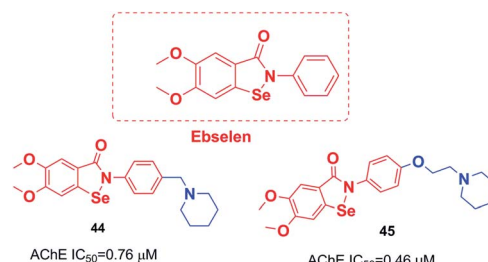
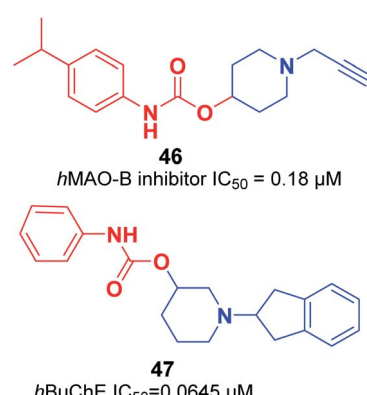
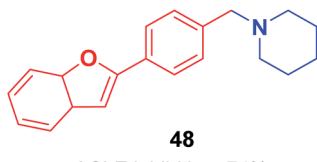


Fig. 23 Ebselen-piperidine hybrids with AChE inhibitor activity.

Fig. 24 *N*-alkylpiperidine carbamates as new inhibitors.



AChE inhibition=74%

Fig. 25 2-Arylbenzofuran derivative anticholinesterase agent.

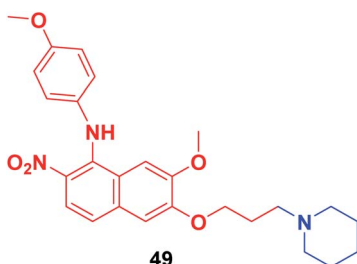
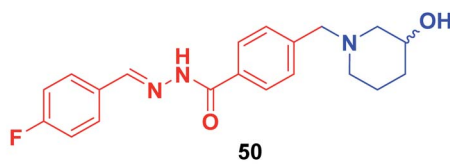
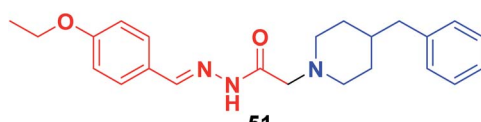
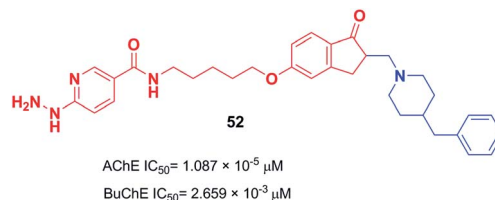
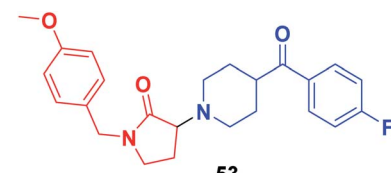
eeAChE $IC_{50}=1.20 \mu\text{M}$
eqBChE $IC_{50}=18.52 \mu\text{M}$

Fig. 26 Structure of 4-N-phenylaminoquinoline-piperidine hybrid.

self-mediated aggregation, as well as metal-chelating ability. Benzimidazole hybrid **29** exhibited greater inhibition of Cu-induced aggregation of $\text{A}\beta_{1-42}$ as well as enhanced antioxidant capacity (Fig. 13)⁴⁰ based on the molecular docking assessment with compound **29** superimposed in the CAS as compared with donepezil. Recently, Chaves *et al.* synthesized 2-hydroxyphenyl benzimidazole derivative **30**. They illustrated that the fluorine atoms and hydroxy groups on the benzene ring resulted in higher cholinergic AChE activity and increased β -amyloid ($\text{A}\beta$) aggregation (self-induced 61%, Cu-induced 71%) (Fig. 13).⁴¹

Mo *et al.* reported the synthesis of benzylpiperidine-linked 1,3-dimethylbenzimidazolinones. The synthesized compounds **31a** and **31b** containing F or Br on the meta-position of the benzyl ring showed submicromolar IC_{50} values for AChE and BuChE. Additionally, these compounds demonstrated a neuroprotective

eeAChE $IC_{50}=8.65 \mu\text{M}$ AChE $IC_{50}=53.1 \mu\text{M}$
BuChE $IC_{50}=67.3 \mu\text{M}$ Fig. 27 Structure of aryl acyl hydrazones based on *N*-benzylpiperidine.AChE $IC_{50}=1.087 \times 10^{-5} \mu\text{M}$
BuChE $IC_{50}=2.659 \times 10^{-3} \mu\text{M}$ Fig. 28 Structure of donepezil-hydrazine nicotinate hybrid **52**.AChE $IC_{50}=0.018 \mu\text{M}$ Fig. 29 Structure of *N*-benzylated-pyrrolidin-2-one-piperidine hybrid **53**.

impact upon H_2O_2 -induced oxidative damage to PC12 cells as well as antioxidant activity based on the DPPH assay (Fig. 14).⁴²

Kilic and colleagues focused on pyridazine derivatives. First, they synthesized 6-chloro-*N*-(2-substituted ethyl)pyridazine-3-carboxamide intermediates from 6-chloropyridazine-3-carboxylic acid and ethylamine derivatives. Next, they employed the Suzuki cross-coupling reaction for the carboxamide intermediate with a suitable phenylboronic acid derivative to obtain the corresponding *N*-(2-substituted ethyl)-6-phenylpyridazine-3-carboxamide derivatives. The biological assay revealed that pyridazine-3-carboxamide derivative **32** exerted dual cholinesterase inhibitory effects, with an IC_{50} of 0.16 μM for AChE and IC_{50} of 9.80 μM for BuChE (Fig. 15).⁴³ The molecular docking presents the interactions of a pyridazine ring with the active-site gorge of AchE and the Trp279 residue in the peripheral anionic site and an anisole ring with a water molecule.

Vila *et al.* reported synthesizing donepezil analogs using a phthalazin-1(2*H*)-one scaffold as potent human ChEIs. The biological assessment showed that the ChE inhibitory potency and selectivity of AChE/BuChE were affected by the structural modifications to a great extent. Also, the length of the chain between the *N*-benzylpiperidine fragment and the

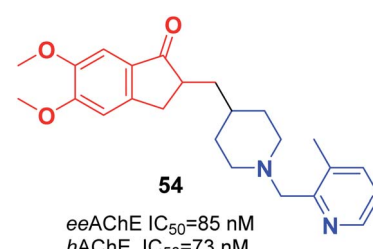
eeAChE $IC_{50}=85 \text{ nM}$
hAChE, $IC_{50}=73 \text{ nM}$

Fig. 30 Structure of a 3-hydroxypyridinaldoxime-indanone derivative.



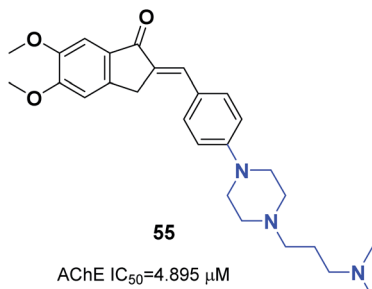


Fig. 31 Structure of indenone-piperazine hybrid 55.

phthalazinone moiety impacted the inhibition of AChE. Compound 33 behaved as a dual cholinesterase inhibitor towards the AChE and BuChE enzymes (Fig. 16).⁴⁴

In 2019, Greunen *et al.* attached the indanone part of donepezil to different commercial heterocycle amines under mild conditions in the presence of catalytic 4-(dimethylamino)pyridine (4-DMAP) to obtain carboxamide derivatives in low to good yield. Among the selected targets, 1-benzyl-N-(1-methyl-3-oxo-2-phenyl-2,3-dihydro-1H-pyrazol-4-yl)piperidine-4-carboxamide 34 afforded *in vitro* AChE inhibition with an IC_{50} value of 5.94 μM (Fig. 17).⁴⁵

De Andrade *et al.* replaced the 5,6-dimethoxy-1-indanone moiety of the donepezil structure with triazoles. This change resulted in a reduction in *h*AChE inhibition and an increase in *h*BuChE inhibitor activity. Compound 35 was the most potent (0.17 nM) selective *h*BuChE inhibitor (>58 000-fold) and showed no cytotoxicity (Fig. 18).⁴⁶

In 2019, El-Sayed constructed pyrrolizine-benzylpiperidine hybrids. *In vitro* assay indicated that in this series, *N*-(1-benzylpiperidin-4-yl)-4-oxo-4,5,6,7-tetrahydro-3*H*-pyrimido[5,4-*a*]pyrrolizine-9-carboxamide 36 exhibited dual inhibitory impact upon *h*AChE and *h*BuChE in the submicromolar range. Also, compound 36 demonstrated cytotoxicity lower or similar to that of donepezil against a normal human hepatic (THLE2) cell line and human neuroblastoma (SH-SY5Y). Based on *in vivo* studies, the compound decreased the cognitive dysfunction of scopolamine-induced AD mice (Fig. 19).⁴⁷

3.3.3. Replacement of indanone with isoxazole and oxadiazole derivatives.

The synthesis and design of novel donepezil

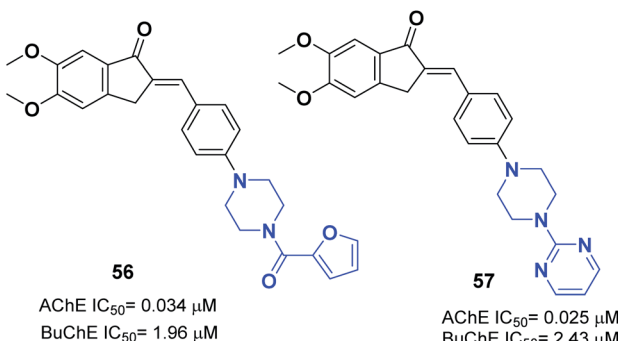


Fig. 32 The structure of piperazin-benzylidene hybrids.

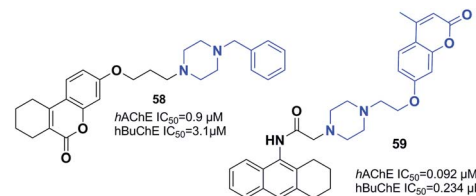


Fig. 33 Structure of chromene/coumarin-piperazine hybrids.

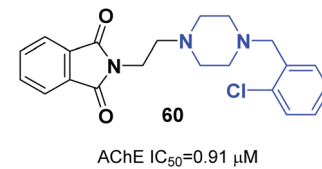


Fig. 34 Structure of phthalimide-piperazine hybrid 60.

hybrids were performed by Saeedi *et al.*, where *N*-benzylpiperidine attached arylated isoxazole through a carboxamide linker. *In vitro* biological assessment showed that the synthetic compounds acted as multi-target ligands and, among them, *N*-(1-benzylpiperidin-4-yl)-5-(3-nitrophenyl)isoxazol-3-carboxamide 37 was the most optimal AChEI ($IC_{50} = 16.07 \mu M$ for AChE; $IC_{50} = 15.16 \mu M$ for BuChE) (Fig. 20).⁴⁸ Tripathi *et al.* connected *N*-benzylpiperidine and 5-phenyl-1,3,4-oxadiazole hybrids with $-NH$ and $-NHCH_2$ linkers to synthesize multi-target hybrids. They found that the binding affinity was enhanced toward the PAs by the presence of 1,3,4-oxadiazole, and was responsible for the extension of the *N*-benzylpiperidine moiety deeper into the CAS of AChE and BuChE, which yielded viable dual inhibitors of ChE. Among the tested compounds, 38 and 39 displayed outstanding inhibition toward *h*AChE, *h*BuChE, and β -secretase-1 (hBACE-1). The anti- $A\beta$ aggregatory activity of 38 was confirmed by the morphological property of incubated samples of $A\beta$ aggregates in the absence

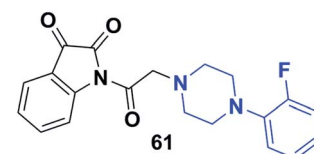


Fig. 35 Structure of (1-(2-(4-(2-fluorobenzyl)piperazin-1-yl)acetyl)indoline-2,3-dione) 61.

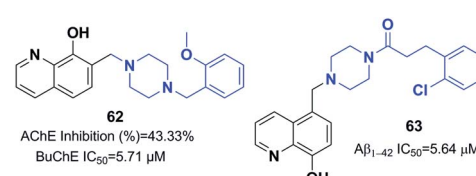


Fig. 36 Structure of 8-hydroxyquinoline-donepezil-like molecules.

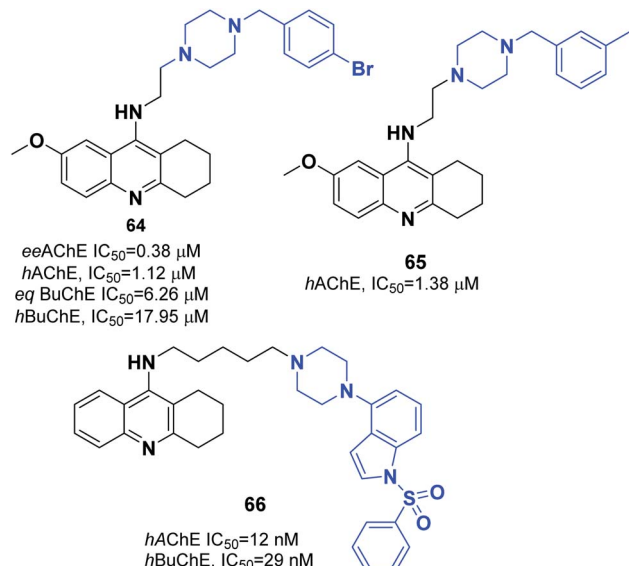


Fig. 37 Structure of acridine-piperazine hybrids.

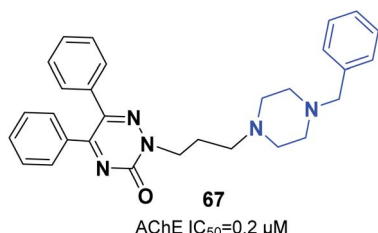


Fig. 38 Structure of 3-oxo-1,2,4-triazine-piperazine hybrid 67.

or presence of an inhibitor (Fig. 20). Compounds **38** and **39** lacked neurotoxicity towards the SH-SY5Y neuroblastoma cell line according to the MTT assay.⁴⁹

3.3.4. Replacement of indanone with thiazole derivatives. Shidore *et al.* prepared diarylthiazole-benzylpiperidine hybrids and assessed their potential in AD treatment using various *in*

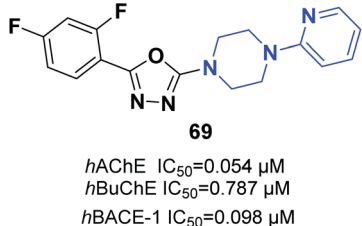
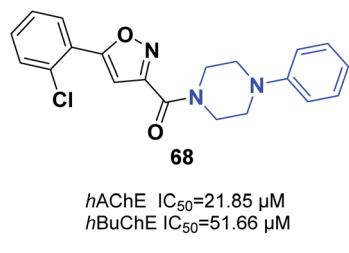


Fig. 39 Isoxazole/oxazole-piperazine hybrids.

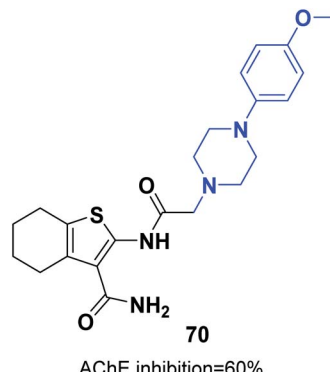
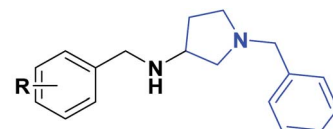


Fig. 40 Structure of thiophene-piperazine 70.



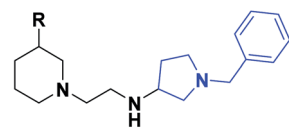
R= 4-OCF₃ **71a**
AChE $IC_{50}=0.058 \mu\text{M}$
BuChE $IC_{50}=0.082 \mu\text{M}$
BACE-1 $IC_{50}=0.115 \mu\text{M}$

R= 2,4 di-F₂ **71b**
AChE $IC_{50}=0.069 \mu\text{M}$
BuChE $IC_{50}=0.127 \mu\text{M}$
BACE-1 $IC_{50}=0.097 \mu\text{M}$

Fig. 41 Structure of benzylamine-pyrrolidine derivative 71.

vitro and *in vivo* experiments. Compound **40** exhibited the greatest inhibitory potency against AChE and BuChE and a mixed-type inhibition of AChE through binding to the PAS and CAS. This derivative also demonstrated reasonably acceptable inhibition of A_β₁₋₄₂ aggregation induced by AChE (27% inhibition) (Fig. 21).⁵⁰ Glycogen synthase kinase-3β (GSK-3β) can be used as an indication that clinical efficacy has been achieved.

Recently, the design and synthesis of new types of pyridinethiazole with benzylpiperidine hybrids were carried out as GSK-3β/AChE dual-target inhibitors. Among these scaffolds, **41** was the most encouraging choice, with an IC_{50} of 0.3 μM for hAChE and IC_{50} of 0.003 μM for hGSK-3β (Fig. 21).⁵¹ The Greunen group synthesized 1-benzyl-N-(5,6-dimethoxy-8H-indeno[1,2-d]thiazol-2-yl) piperidine-4-carboxamide **42**, which exhibited AChE inhibitory activity ($IC_{50} = 0.41 \mu\text{M}$) (Fig. 21).⁴⁵



72a R=Ph BuChE $IC_{50}=2.39 \mu\text{M}$
72b R=CH₂Ph BuChE $IC_{50}=1.94 \mu\text{M}$

Fig. 42 Structure of piperazine-benzyl pyrrolidine derivatives.

Table 1 Summary of multi-target-directed ligands

| Compound number | AChE | BuChE | Inhibition of A β | BACE-1 | Metal chelation | MAO | Non-toxicity | Reference |
|-----------------|------|-------|-------------------------|--------|-----------------|-----|--------------|-----------|
| 1 | * | | | * | | | | 14 |
| 2 | * | | | * | | | | 14 |
| 3 | * | | | | | | | 15 |
| 4 | * | * | * | | | | | 16 |
| 5 | * | * | | | | * | | 17 |
| 6 | * | * | | | | | | 18 |
| 7 | * | | * | * | | | | 19 |
| 8 | * | | * | * | | | | 19 |
| 9 | * | | * | | * | | * | 21 |
| 10 | * | * | | | | | | 22 |
| 11 | | * | | | | | | 23 |
| 12 | * | * | * | | | | | 22 |
| 13 | * | * | | | | | | 24 |
| 14 | * | * | | | | * | * | 25 |
| 15 | * | | | | | * | | 26 |
| 16 | * | | | | | | | 27 |
| 17 | * | | * | | | * | * | 28 |
| 18 | * | * | | | | * | | 29 |
| 19 | * | | | | | | | 30 |
| 20 | * | * | * | | | | | 31 |
| 21 | * | * | * | | * | * | * | 32 |
| 22 | * | * | | | | | | 33 |
| 23 | * | * | | | | | | 34 |
| 24 | * | * | | | * | | | 35 |
| 25 | * | * | | | * | | | 36 |
| 26 | * | | | | | | | 37 |
| 27 | * | * | * | | * | | * | 38 |
| 28 | * | * | | | * | | * | 39 |
| 29 | * | | * | | * | | | 40 |
| 30 | * | | * | | | | | 41 |
| 31 | * | * | | | | | | 42 |
| 32 | * | * | | | | | | 43 |
| 33 | * | * | | | | | | 44 |
| 34 | * | | | | | | | 45 |
| 35 | | * | | | | | | 46 |
| 36 | * | * | | | | | * | 47 |
| 37 | * | * | | | | | | 48 |
| 38 | * | * | * | | * | | * | 49 |
| 39 | * | * | * | | * | | * | 49 |
| 40 | * | * | | | * | | | 50 |
| 41 | * | | | | | | | 51 |
| 42 | * | | | | | | | 45 |
| 43 | * | * | | | | | | 52 |
| 44 | * | | | | | | | 54 |
| 45 | * | | | | | | | 54 |
| 46 | | | | | | | * | 17 |
| 47 | | * | | | | | | 17 |
| 48 | * | | | | | | | 55 |
| 49 | * | * | | | | | | 56 |
| 50 | * | | | | | | | 57 |
| 51 | * | * | | | | | | 58 |
| 52 | * | * | | | | | | 59 |
| 53 | * | | | | | | | 60 |
| 54 | * | | * | | | | | 61 |
| 55 | * | | | | | | * | 62 |
| 56 | * | * | * | | | | | 63 |
| 57 | * | * | * | | | | | 63 |
| 58 | * | * | | | | | | 64 |
| 59 | * | * | * | | * | | | 65 |
| 60 | * | | | | | | | 66 |
| 61 | * | | | | | | | 67 |
| 62 | * | * | * | | | | * | 68 |
| 63 | | | * | | * | | | 69 |



Table 1 (Contd.)

| Compound number | AChE | BuChE | Inhibition of A β | BACE-1 | Metal chelation | MAO | Non-toxicity | Reference |
|-----------------|------|-------|-------------------------|--------|-----------------|-----|--------------|-----------|
| 64 | * | * | | | | | | 70 |
| 65 | * | | | | | | | 71 |
| 66 | * | * | | | | | | 72 |
| 67 | * | | | | | | | 73 |
| 68 | * | * | | | | | | 74 |
| 69 | * | * | | * | | | * | 75 |
| 70 | * | | | | | | | 76 |
| 71 | * | * | | * | | | | 77 |
| 72 | | * | * | * | | | | 78 |

3.4. Replacement of indanone with a lipophilic structure

Estrada *et al.* combined the lipoic acid structure with *N*-benzylpiperidine to obtain novel MTDLs. Lipoic acid-based hybrids were synthesized through coupling reaction between the corresponding amine derivative and (*R,S*)-LA or enantiopure (*R*)-LA or (*S*)-LA in a microwave oven at 120 °C, using 1,1'-carbonoyldiimidazole (CDI) as an activating agent. The most potent ligand **43** demonstrated significant inhibitory activity against ChEs (Fig. 22).⁵²

3.5. Miscellaneous MTDLs

An organoselenium compound with biological properties is ebselen (2-phenyl-1,2-benziselenazol-3(2H)-one).⁵³ Luo *et al.* connected ebselen to the pharmacophores of the AChEIs for producing novel hybrid molecules. Compounds **44** and **45** exhibited the highest potency against AChE (Fig. 23).⁵⁴

Košák *et al.* developed a class of *N*-alkylpiperidine carbamates as viable agents against AD, with the most promising compounds being **46** and **47**. *N*-Propargylpiperidine **46** revealed *h*MAO-B inhibitor activity ($IC_{50} = 0.18 \mu\text{M}$), and compound **47** acted as a selective *h*BuChE inhibitor with an IC_{50} of 0.0645 μM (Fig. 24).¹⁷

Pouramiri *et al.* synthesized a library of 2-aryl benzofuran derivatives through four-step reactions from 2-hydroxybenzyl alcohol in good yield. In comparison with donepezil, the synthesized compound **48** with the piperidine moiety exhibited the most optimal AChE inhibition activity of 74% at 23 μM (Fig. 25).⁵⁵

Cai *et al.* investigated the role of the 4-*N*-phenylaminoquinoline core in AChE and BuChE inhibition. They synthesized a series of novel derivatives of 4-methyl-piperidine-4-*N*-phenylaminoquinoline from the commercially available vanillic acid *via* ten steps. The biological evaluation indicated that compound **49** with a *para* methoxy group was more highly potent against AChE than galanthamine (Fig. 26).⁵⁶

In 2018, the synthesis of a novel series of aryl acyl hydrazones was carried out by Viegas *et al.* according to the pharmacophoric *N*-benzyl-piperidine subunit of donepezil, the substituted hydroxy-piperidine fragment, and an acyl hydrazone linker. Among *N*-benzyl-piperidine acyl hydrazone derivatives, compound **50** showed satisfactory inhibition of electric eel (*Electrophorus electricus*) AChE, COX-1 (64%), and COX-2 (53%) (Fig. 27).⁵⁷ Özer *et al.* carried out the synthesis of *N*²-2-(4-

benzylpiperidin-1-yl)acyl hydrazone derivatives. Based on the enzyme inhibition assay results, compound **51** with the 4-ethoxybenzylidene group was the most active, with an IC_{50} of 53.1 μM for AChE enzyme and IC_{50} of 67.3 μM BuChE enzyme (Fig. 27).⁵⁸

The design and the synthesis of donepezil-hydrazine nicotinates were performed by Zurek *et al.* in 2013. All the products showed a higher affinity for AChE than BuChE. Compound **52** was the most effective inhibitor of AChE ($IC_{50} = 1.087 \times 10^{-5} \mu\text{M}$). The molecular modeling was performed using Cache software and showed that compound **52** binds to AChE with a total score of -181.939 (Fig. 28).⁵⁹

Gupta *et al.* replaced the 1-indanone moiety with *N*-benzylated-pyrrolidin-2-one and found that 3-(4-(4-fluorobenzoyl)-piperidin-1-yl)-1-(4-methoxybenzyl)-pyrrolidin-2-one **53** exhibited an excellent anti-Alzheimer's profile (Fig. 29).⁶⁰

Wang *et al.* focused on modifying the benzyl group of donepezil using several disparate fragments, including quinolone, pyridine, and hydroxyquinoline, for better interaction with dual binding sites of AChE. Based on the screening results, all the compounds demonstrated a potent AChE inhibition with values of IC_{50} in the nanomolar range, satisfactory antioxidant activities, A β interaction, and BBB penetration. (5,6-dimethoxy-2-((1-((3-methylpyridin-2-yl)methyl)piperidin-4-yl)methyl)-2,3-dihydro-1*H*-inden-1-one) **54** displayed outstanding inhibition of AChE, satisfactory metal chelation, and inhibitory impact upon self-induced (18.5%), *h*AChE-induced (72.4%), and Cu²⁺-induced (46.3%) aggregation of A β ₁₋₄₂ at 20 μM (Fig. 30).⁶¹

4. Derivatives with replacement of the piperidine part of donepezil

4.1. Indanone-piperazine hybrids

The *N*-substituted piperazine moiety mimics the *N*-benzylpiperidine fragment from donepezil. In 2016, Saglik and coworkers synthesized novel donepezil analogs by replacing the piperidine part with 4-substituted piperazines. Among the compounds, 4-dimethylamino piperazine derivative **55** displayed prominent inhibition of AChE and nontoxicity towards the NH3T3 cell line (Fig. 31).⁶²

In 2017, Mishra attached the indanone part of donepezil to the 4-substituted piperazin-1-yl-benzylidene moiety from



commercially available substituted piperazine and 4-fluoro benzaldehyde at 100 °C followed by the Knoevenagel condensation reaction to link the indanone moiety with various substituted piperazines through a methylene linker. Compounds **56** and **57** displayed excellent AChE inhibitory ability with an $IC_{50} = 0.034 \mu\text{M}$ and $0.025 \mu\text{M}$ and $\text{A}\beta$ fibril aggregation inhibition activity of 80.4 and 81.6%, respectively (Fig. 32).⁶³

4.2. O-Heterocycle-piperazine hybrids

Gulcan designed and synthesized *6H*-benzo[*c*]chromen-6-one and 7,8,9,10-tetrahydro-benzo[*c*]chromen-6-one derivatives (Fig. 33).⁶⁴ Replacement of indanone with chromene and piperidine with piperazine led to an increase in the inhibitory activity of compound **58**. In addition, a three-carbon atom spacer between the benzo[*c*]chromen-6-one moiety and piperazine is ideal for cholinesterase inhibition within this group of compounds.

Tacrine is another FDA-approved ChE inhibitor that has become an extensively used scaffold in recent years. In 2013, Xie *et al.* synthesized a novel MTDL by connecting tacrine, coumarins, and piperazine. Among the synthetic compounds, **59** with the methyl on the 4-position of chromene showed the greatest AChE inhibition, and an acceptable BuChE inhibition and $\text{A}\beta$ aggregation inhibition (67.8%, 20 μM). Moreover, **59** was a satisfactory metal chelator. Based on molecular modeling and kinetic studies, **59** was a mixed type of inhibitor that binds to the CAS, PAS, and mid-gorge site of AChE at the same time (Fig. 33).⁶⁵

4.3. N-Heterocycle-piperazine hybrids

Mohammadi *et al.* designed phthalimid-piperazine scaffolds. They employed the Gabriel synthetic reaction of phthalic anhydride with *N*-aminoethylpiperazine to obtain 2-(2-(piperazin-1-yl)ethyl)isoindoline-1,3-dione with 61% yield. In addition, equimolar quantities of isoindoline derivatives were reacted with the appropriate benzyl chloride to obtain the corresponding targets. Biological assessment of anticholinesterase activity determined that products with electron-withdrawing groups showed greater potency, and compound **60** with a chloro substituent on the *ortho* position of the phenyl ring exhibited the greatest AChE inhibition with an IC_{50} of 0.91 μM (Fig. 34).⁶⁶

Replacement of the indanone part of donepezil with indoline-2,3-dione generated a novel scaffold with greater activity than that of donepezil. Compound **61** (1-(2-(4-(2-fluorobenzyl)piperazin-1-yl)acetyl)indoline-2,3-dione) demonstrated greater inhibitory activity compared to donepezil because of the 2-fluorobenzyl replacement and the acetamido spacer. This molecule remarkably binds to the H-bond receptor with Phe288, leading to more optimal pharmacological activity (Fig. 35).⁶⁷

Prati *et al.* proposed and designed a new series of 8-hydroxyquinoline-donepezil-like hybrids with multi-targeting activities towards key AD targets. The new hybrid 7-((4-(2-methoxybenzyl)piperazin-1-yl)methyl)-8-hydroxyquinoline **62** inhibited $\text{A}\beta$ self-aggregation, exhibited the highest potency for chelating copper(II) and zinc(II), and exerted the highest *in vitro* antioxidant activity. For compound **62**, significant BBB penetration, negligible cytotoxicity in T67 cells, and acceptable toxicity in primary human umbilical vein endothelial cells

(HUVECs) accompanied its multi-target profile (Fig. 36).⁶⁸ The interaction of 8-hydroxyquinoline and donepezil hybrid molecules with cholinesterase and monoamine oxidase enzymes was evaluated by Yang *et al.*⁶⁹ Compound **63** had considerable inhibitory impacts against self-induced aggregation of $\text{A}\beta_{1-42}$ ($IC_{50} = 5.64 \mu\text{M}$) and potential antioxidant properties (2.63 Trolox equivalents) (Fig. 36). Furthermore, **63** was capable of chelating biometals, inhibiting aggregation of $\text{Cu}^{2+}/\text{Zn}^{2+}$, and penetrating the BBB *in vitro*.

Korabecny developed novel ChEIs based on 7-methoxytacrine-donepezil-like structures. The synthesized compounds showed cholinesterase inhibitory activity, and the values of IC_{50} were in the micromolar to sub-micromolar scale range toward enzymes of human and animal origin. *N*-(2-{4-[(4-Bromophenyl)methyl]piperazin-1-yl}ethyl)-7-methoxy-1,2,3,4-tetrahydroacridin-9-amine trihydrochloride **64** was the most promising compound (Fig. 37).⁷⁰ In 2016, Sepsova *et al.* evaluated the interaction of 7-methoxy-*N*-(2-(4-(3-methyl benzyl)piperazin-1-yl)ethyl)-1,2,3,4-tetrahydroacridin-9-amine with AChE and cholinergic (muscarinic and nicotinic) receptors. The results showed that compound **65** acts as an AChE inhibitor (Fig. 37).⁷¹ Więckowska *et al.* designed (phenyl sulfonyl-1*H*-indol-4-yl piperazin-1-yl)hexyl)-1,2,3,4-tetrahydroacridin-9-amine, and biological evaluation indicated that compound **66** had a HT6 antagonist ($K_b = 27 \text{ nM}$) (Fig. 37).⁷²

Molecular hydrides of the 5,6-biphenyl-3-oxo-1,2,4-triazine nucleus and substituted piperazines were synthesized and assessed for inhibition of ChE. Compound **67** (5,6-diphenyl-3-oxo-2-(3-(4-benzylpiperazin-1-yl)propyl)-1,2,4-triazine) with three carbon atoms connected to the benzylpiperazine terminal group demonstrated inhibition potency toward AChE with an IC_{50} of 0.2 μM . Based on docking models, the benzyl group engaging at the lowest part of the enzyme gorge plays a crucial role in interaction with CAS residues of AChE (Fig. 38).⁷³

4.4. Isoxazole/oxazole–piperazine hybrids

Saeedi and colleagues designed new isoxazoles linked to the moiety of phenylpiperazine and evaluated the AChE inhibitory effect of targets through Ellman's method as compared to donepezil and rivastigmine references. Among the synthetic compounds, (5-(2-chlorophenyl)isoxazol-3-yl)(4-phenylpiperazin-1-yl)methanone **68** was the most potent candidate (Fig. 39).⁷⁴ Tripathi *et al.* explored the synthesis of 2-pyridylpiperazine hybrids and 5-phenyl-1,3,4-oxadiazoles with considerable inhibitory possibilities for AD. Compound **69** with a 2,4-difluoro replacement at the end phenyl ring was considered the most viable lead, with cholinesterase inhibition and β -secretase-1 activity. Based on an analysis of enzyme kinetics, **69** demonstrated a mixed-type inhibition toward *hAChE*, with a K_i of 0.030 μM . Compound **69** showed considerable deposition of propidium iodide from the PAS of *hAChE*, penetration in PAMPA, neuroprotective capability against the SH-SY5Y neuroblastoma cell line, and outstanding BBB (Fig. 39).⁷⁵

4.5. Thiophene–piperazine hybrids

The synthesis of new thiophene derivatives and evaluation of their biological inhibition were carried out by Ismail *et al.* 2-(2-



(4-(4-Methoxyphenyl)piperazin-1-yl)acetamido)-4,5,6,7-tetrahydrobenzo[*b*]thiophene-3-carboxamide **70** demonstrated inhibition of 60% in comparison with only 40% inhibition for donepezil (Fig. 40).⁷⁶ The amide linker in this scaffold led to extra binding to the receptor through three different H-bonds with Phe288 and resulted in increased pharmacological activity.

4.6. Modified scaffolds based on pyrrolidine

One of the latest studies on MTDLs was carried out by Choube *et al.* They designed derivatives of *N*-benzyl pyrrolidine and biologically assessed their ability to treat AD. Among the synthesized leads, **71a** and **71b** demonstrated proportionate enzymatic inhibition against cholinesterases. They also showed significant PAS-AChE binding ability, outstanding BBB permeation, neuroprotective activity against A β -induced stress, and possible disassembly of A β aggregates (Fig. 41).⁷⁷

Wichur *et al.* synthesized novel multifunctional ligands to investigate their inhibitory effects on BuChE, β -secretase, and amyloid- β (A β), and their antioxidant, aggregation of tau protein, and metal-chelating characteristics. All the targets exhibited dual anti-aggregating properties towards A β and tau protein (**72a**: 45% for A β , 53% for tau; **72b**: 49% for A β , 54% for tau). Compound **72a** with an IC₅₀ of 2.39 μ M and **72ab** with an IC₅₀ of 1.94 μ M exhibited the highest inhibitory potency against BuChE (Fig. 42).⁷⁸

5. Conclusion

The enhancement of ACh would be considered an effective method to compensate for the deficiency of acetylcholine, and most treatment strategies for AD are focused on enhancing cholinergic neurotransmission. However, there are severe side effects to FDA-approved drugs for AD, including vomiting, nausea, diarrhea, bradycardia, abnormal dreams, and fatigue. Because of AD's complex pathophysiology, there is an urgent need to discover and develop efficient new therapeutic agents with minimal side effects to effectively combat AD.

In this review, we discussed the structural modification of donepezil as described in articles published from 2012–2020. This review is categorized into sections according to the changes made to the donepezil linker, replacement of the indanone moiety with O-containing heterocycles or N-heterocyclic moieties, and replacement of the piperidine moiety with piperazine or pyrrolidine structures. In addition, we tried to outline different synthetic small molecules based on the structure of donepezil and describe detailed structure–activity relationships.

Studies showed that attaching chromones with piperidine will produce ChE inhibitors and selective hMAO inhibition. Also, the type of spacer modulates additional activities, including metal-chelating characteristics. Furthermore, using hydroxyquinoline instead of the indanone part of donepezil leads to multi-target properties. Hybrid molecules from tetrahydroacridin-9-amines and piperazine will exhibit the best dual ChE activities and are vital for the effective treatment of AD. This review will assist researchers and medicinal chemists in designing novel, target-based, and advanced donepezil

analogs with advantageous biological properties for effective AD therapy (Table 1).

Abbreviations

| | |
|---------------|---|
| ABTS | (2,2'-Azino-bis(3-ethylbenzothiazoline-6-sulfonic acid) |
| ACh | Acetylcholine |
| AChE | Acetylcholinesterase |
| AChEI | Acetylcholinesterase inhibitor |
| AD | Alzheimer's disease |
| BACE-1 | β -Secretase-1 |
| BuChE | Butyrylcholinesterase |
| CAS | Catalytic anionic site |
| ChE | Cholinesterase |
| DFH | Donepezil–flavonoid hybrid |
| eeAChE | <i>Electrophorus electricus</i> acetylcholinesterase |
| FRAP | Ferric reducing antioxidant power |
| Glu | Glutamate |
| GSK-3 β | Glycogen synthase kinase-3 β |
| His | Histidine |
| 5-HT | 5-Hydroxytryptamine (serotonin) |
| 5-LOX | 5-Lipoxygenase |
| MAO | Monoamine oxidase |
| MAOI | Monoamine oxidase inhibitor |
| MTDL | Multitarget-directed ligand |
| PAS | Peripheral anionic site |
| Phe | Phenylalanine |
| QSAR | Quantitative structure–activity |
| SI | Selectivity index |
| σ -1R | Sigma-1 receptor |
| Trp | Tryptophan |

Conflicts of interest

There are no conflicts to declare.

References

- 1 P. Scheltens, B. De Strooper, M. Kivipelto, H. Holstege, G. Chételat, C. E. Teunissen, J. Cummings and W. M. van der Flier, *Lancet*, 2021, **397**, 1577–1590.
- 2 E. Scarpini, P. Scheltens and H. Feldman, *Lancet Neurol.*, 2003, **2**, 539–547.
- 3 V. N. Talesa, *Mech. Ageing Dev.*, 2001, **122**, 1961–1969.
- 4 X. Huang, R. D. Moir, R. E. Tanzi, A. I. Bush and J. T. Rogers, *Ann. N. Y. Acad. Sci.*, 2004, **1012**, 153–163.
- 5 P. Seeman and N. Seeman, *Synapses*, 2011, **1297**, 1289–1297.
- 6 M. Coedert, M. C. Spillantini, D. Rutherford and R. A. Crowther, *Neuron*, 1989, **3**, 519–526.
- 7 P. T. Francis, A. M. Palmer, M. Snape and G. K. Wilcock, *J. Neurol., Neurosurg. Psychiatry*, 1999, **66**, 137–147.
- 8 T. L. Rosenberry, X. Brazzolotto, I. R. MacDonald, M. Wandhammer, M. Trovaslet-Leroy, S. Darvesh and F. Nachon, *Molecules*, 2017, **22**, 1–21.
- 9 M. Rodrigues Simoes, F. Dias Viegas, M. Moreira, M. Freitas Silva, M. Riquiel, P. da Rosa, M. Castelli, M. dos Santos,





M. Soares and C. Viegas, *Mini-Rev. Med. Chem.*, 2014, **14**, 2–19.

10 J. Cheung, M. J. Rudolph, F. Burshteyn, M. S. Cassidy, E. N. Gary, J. Love, M. C. Franklin and J. J. Height, *J. Med. Chem.*, 2012, **55**, 10282–10286.

11 H. Sugimoto, Y. Yamanishi, Y. Iimura and Y. Kawakami, *Curr. Med. Chem.*, 2000, **7**, 303–339.

12 S. Uddin, A. Al Mamun, T. Kabir, G. Ashraf and M. N. Bin-Jumah, *Mol. Neurobiol.*, 2021, **58**, 281–303.

13 S. Maramai, M. Benchekroun, M. T. Gabr and S. Yahiaoui, *BioMed Res. Int.*, 2020, **2020**, 5120230.

14 P. Costanzo, L. Cariati, D. Desiderio, R. Sgammato, A. Lamberti, R. Arcone, R. Salerno, M. Nardi, M. Masullo and M. Oliverio, *ACS Med. Chem. Lett.*, 2016, **7**, 470–475.

15 D. G. Van Greunen, W. Cordier, M. Nell, C. Van Der Westhuyzen, V. Steenkamp, J. Panayides and D. L. Riley, *Eur. J. Med. Chem.*, 2017, **127**, 671–690.

16 J. Yan, J. Hu, A. Liu, L. He, X. Li and H. Wei, *Bioorg. Med. Chem.*, 2017, **25**, 2946–2955.

17 U. Košák, N. Strašek, D. Knez, M. Jukič, S. Žakelj, A. Zahirović, A. Pišlar, X. Brazzolotto, F. Nachon, J. Kos and S. Gobec, *Eur. J. Med. Chem.*, 2020, **197**, 112282.

18 L. Monjas, M. P. Arce, R. León, J. Egea, C. Pérez, M. Villarroya, M. G. López, C. Gil, S. Conde and M. Isabel, *Eur. J. Med. Chem.*, 2017, **130**, 60–72.

19 P. Sharma, A. Tripathi, P. N. Tripathi, S. K. Prajapati, A. Seth, M. K. Tripathi, P. Srivastava, V. Tiwari, S. Krishnamurthy and S. K. Srivastava, *Eur. J. Med. Chem.*, 2019, **167**, 510–524.

20 S. Ou and K. Kwok, *J. Sci. Food Agric.*, 2004, **1269**, 1261–1269.

21 K. S. T. Dias, C. T. de Paula, T. dos Santos, I. N. O. Souza, M. S. Boni, M. J. R. Guimarães, F. M. R. da Silva, N. G. Castro, G. A. Neves, C. C. Veloso, M. M. Coelho, I. S. F. de Melo, F. C. V. Giusti, A. Giusti-Paiva, M. L. da Silva, L. E. Dardenne, I. A. Guedes, L. Pruccoli, F. Morroni, A. Tarozzi and C. Viegas, *Eur. J. Med. Chem.*, 2017, **130**, 440–457.

22 W. Xu, X. B. Wang, Z. M. Wang, J. J. Wu, F. Li, J. Wang and L. Y. Kong, *MedChemComm*, 2016, **7**, 990–998.

23 M. Benchekroun, L. Ismaili, M. Pudlo, V. Luzet, T. Gharbi, B. Refouelet and J. Marco-Contelles, *Future Med. Chem.*, 2015, **7**, 15–21.

24 M. Estrada, C. Herrera-Arozamena, C. Pérez, D. Viña, A. Romero, J. A. Morales-García, A. Pérez-Castillo and M. I. Rodríguez-Franco, *Eur. J. Med. Chem.*, 2016, **121**, 376–386.

25 X. B. Wang, F. C. Yin, M. Huang, N. Jiang, J. S. Lan and L. Y. Kong, *RSC Med. Chem.*, 2020, **11**, 225–233.

26 M. E. Valencia, C. Herrera-arozamena, L. De Andrés, J. A. Morales-garcía, A. Pérez-castillo, E. Ramos, A. Romero, D. Viña, M. Yáñez, E. Laurini, S. Priol and M. I. Rodríguez, *Eur. J. Med. Chem.*, 2018, **156**, 534–553.

27 A. Asadipour, M. Alipour, M. Jafari, M. Khoobi, S. Emami, H. Nadri, A. Sakhteman, A. Moradi, V. Sheibani, F. Homayouni Moghadam, A. Shafiee and A. Foroumadi, *Eur. J. Med. Chem.*, 2013, **70**, 623–630.

28 P. Cai, S. Fang, X. Yang and J. Wu, *ACS Chem. Neurosci.*, 2017, **8**, 2496–2511.

29 J. Joubert, G. B. Foka, B. P. Repsold, D. W. Oliver, E. Kapp and S. F. Malan, *Eur. J. Med. Chem.*, 2017, **125**, 853–864.

30 M. Asadi, M. Ebrahimi, M. Mohammadi-Khanaposhtani, H. Azizian, S. Sepehri, H. Nadri, M. Biglar, M. Amanlou, B. Larijani, R. Mirzazadeh, N. Edraki and M. Mahdavi, *Chem. Biodiversity*, 2019, **16**, e1900370.

31 A. Więckowska, K. Więckowski, M. Bajda, B. Brus, K. Sałat, P. Czerwińska, S. Gobec, B. Filipiak and B. Malawska, *Bioorg. Med. Chem.*, 2015, **23**, 2445–2457.

32 F. Li, Z.-M. Wang, J.-J. Wu, J. Wang, S.-S. Xie, J.-S. Lan, W. Xu, L.-Y. Kong and X.-B. Wang, *J. Enzyme Inhib. Med. Chem.*, 2016, **31**, 41–53.

33 A. Samadi, M. Estrada, C. Pérez, M. I. Rodríguez-franco, I. Iriepa, I. Moraleda, M. Chioua and J. Marco-contelles, *Eur. J. Med. Chem.*, 2012, **57**, 296–301.

34 A. Samadi, M. D. L. F. Revenga, C. Pérez, I. Iriepa, I. Moraleda, M. I. Rodríguez-Franco and J. Marco-Contelles, *Eur. J. Med. Chem.*, 2013, **67**, 64–74.

35 Y. Zhou, W. Sun, J. Peng, H. Yan, L. Zhang, X. Liu and Z. Zuo, *Bioorg. Chem.*, 2019, **93**, 103322.

36 L. Wang, G. Esteban, M. Ojima, O. M. Bautista-Aguilera, T. Inokuchi, I. Moraleda, I. Iriepa, A. Samadi, M. B. H. Youdim, A. Romero, E. Soriano, R. Herrero, A. P. Fernández Fernández, Ricardo-Martínez-Murillo, J. Marco-Contelles and M. Unzeta, *Eur. J. Med. Chem.*, 2014, **80**, 543–561.

37 M. Pudlo, V. Luzet, L. Ismaïli, I. Tomassoli, A. Iutzeler and B. Refouelet, *Bioorg. Med. Chem.*, 2014, **22**, 2496–2507.

38 J. Wang, Z. M. Wang, X. M. Li, F. Li, J. J. Wu, L. Y. Kong and X. B. Wang, *Bioorg. Med. Chem.*, 2016, **24**, 4324–4338.

39 O. M. Bautista-aguilera, G. Esteban, I. Bolea, K. Nikolic, D. Agbaba, I. Moraleda, I. Iriepa, A. Samadi, E. Soriano, M. Unzeta and J. Marco-contelles, *Eur. J. Med. Chem.*, 2014, **75**, 82–95.

40 L. Piemontese, D. Tomás, A. Hiremathad, V. Capriati, E. Candeias, S. M. Cardoso, S. Chaves and M. A. Santos, *J. Enzyme Inhib. Med. Chem.*, 2018, **33**, 1212–1224.

41 S. Chaves, S. Resta, F. Rinaldo, M. Costa, R. Josselin, K. Gwizdala, L. Piemontese, V. Capriati, A. R. Pereira-santos, S. M. Cardoso and M. Am, *Molecules*, 2020, **25**, 985.

42 J. Mo, T. Chen, H. Yang, Y. Guo, Q. Li, Y. Qiao, H. Lin, F. Feng, W. Liu, Y. Chen, Z. Liu and H. Sun, *J. Enzyme Inhib. Med. Chem.*, 2020, **35**, 330–343.

43 B. Kilic, H. O. Gulcan, F. Aksakal, T. Ercetin, N. Oruklu, E. Umit Bagriacik and D. S. Dogruler, *Bioorg. Chem.*, 2018, **79**, 235–249.

44 N. Vila, P. Besada, D. Viña, M. Sturlese, S. Moro and C. Terán, *RSC Adv.*, 2016, **6**, 46170–46185.

45 D. G. van Greunen, C. Johan van der Westhuizen, W. Cordier, M. Nell, A. Stander, V. Steenkamp, J. L. Panayides and D. L. Riley, *Eur. J. Med. Chem.*, 2019, **179**, 680–693.

46 P. de Andrade, S. P. Mantoani, P. S. Gonçalves Nunes, C. R. Magadán, C. Pérez, D. J. Xavier, E. T. S. Hojo, N. E. Campillo, A. Martínez and I. Carvalho, *Bioorg. Med. Chem.*, 2019, **27**, 931–943.

47 N. A. E. El-Sayed, A. E. S. Farag, M. A. F. Ezzat, H. Akincioglu, İ. Gülcin and S. M. Abou-Seri, *Bioorg. Chem.*, 2019, **93**, 103312.

48 M. Saeedi, P. Felegari, A. Iraji, R. Hariri, A. Rastegari, S. S. Mirfazli, N. Edraki, O. Firuzi, M. Mahdavi and T. Akbarzadeh, *Arch. Pharm.*, 2020, **1**–12.

49 P. Sharma, A. Tripathi, P. N. Tripathi, S. Sen Singh, S. P. Singh and S. K. Shrivastava, *ACS Chem. Neurosci.*, 2019, **10**, 4361–4384.

50 M. Shidore, J. Machhi, K. Shingala, P. Murumkar, M. K. Sharma, N. Agrawal, A. Tripathi, Z. Parikh, P. Pillai and M. R. Yadav, *J. Med. Chem.*, 2016, **59**, 5823–5846.

51 X. Jiang, Y. Wang, C. Liu, C. Xing, Y. Wang, W. Lyu, S. Wang, Q. Li, T. Chen, Y. Chen, F. Feng, W. Liu and H. Sun, *Bioorg. Med. Chem.*, 2021, **30**, 115940.

52 M. Estrada, C. Pérez, E. Soriano, E. Laurini, M. Romano, S. Pricl, J. A. Morales-García, A. Pérez-Castillo and M. I. Rodriguez-Franco, *Future Med. Chem.*, 2016, **8**, 1191–1207.

53 T. Schewe, *Gen. Pharmacol.*, 1995, **26**, 1153–1169.

54 Z. Luo, L. Liang, J. Sheng, Y. Pang, J. Li, L. Huang and X. Li, *Bioorg. Med. Chem.*, 2014, **22**, 1355–1361.

55 B. Pouramiri, M. Mahdavi, S. Moghimi, L. Firoozpour, H. Nadri, A. Moradi, E. Tavakolinejad-Kermani, A. Asadipour and A. Foroumadi, *Lett. Drug Des. Discovery*, 2016, **13**, 897–902.

56 R. Cai, L. N. Wang, J. J. Fan, S. Q. Geng and Y. M. Liu, *Bioorg. Chem.*, 2019, **93**, 103328.

57 F. Pereira, D. Viegas, M. D. F. Silva, M. Divino, R. Castelli, M. M. Riquiel, R. P. Machado, S. Macedo, D. Oliveira, É. P. Morais, V. S. Gontijo, F. M. R. Silva, D. D. Alincourt, N. G. Castro, A. Gilda, A. Giusti-paiva, F. C. Vilela, L. Orlandi, M. P. Veloso, L. Felipe, L. Coelho, M. Ionta, W. De Oliveira, C. Junior, P. Maria and Q. Bellozi, *Eur. J. Med. Chem.*, 2018, **147**, 48–65.

58 E. Özturan Özer, O. Unsal Tan, K. Ozadali, T. Küçükkilinç, A. Balkan and G. Uçar, *Bioorg. Med. Chem. Lett.*, 2013, **23**, 440–443.

59 E. Żurek, P. Szymański and E. Mikiciuk-Olasik, *Drug Res.*, 2013, **63**, 137–144.

60 M. Gupta, M. Ojha, D. Yadav, S. Pant and R. Yadav, *ACS Chem. Neurosci.*, 2020, **11**, 2849–2860.

61 Z. M. Wang, P. Cai, Q. H. Liu, D. Q. Xu, X. L. Yang, J. J. Wu, L. Y. Kong and X. B. Wang, *Eur. J. Med. Chem.*, 2016, **123**, 282–297.

62 B. N. Sağlık, S. İlgin and Y. Özkar, *Eur. J. Med. Chem.*, 2016, **124**, 1026–1040.

63 C. B. Mishra, S. Kumari, A. Manral, A. Prakash, V. Saini, A. M. Lynn and M. Tiwari, *Eur. J. Med. Chem.*, 2017, **125**, 736–750.

64 H. O. Gulcan, S. Unlu, I. Esiringu, T. Ercetin, Y. Sahin, D. Oz and M. F. Sahin, *Bioorg. Med. Chem.*, 2014, **22**, 5141–5154.

65 S. S. Xie, X. B. Wang, J. Y. Li, L. Yang and L. Y. Kong, *Eur. J. Med. Chem.*, 2013, **64**, 540–553.

66 A. Mohammadi-farani, A. Ahmadi, H. Nadri and A. Aliabadi, *Daru, J. Pharm. Sci.*, 2013, **21**, 47–56.

67 M. M. Ismail, M. M. Kamel, L. W. Mohamed and S. I. Faggal, *Molecules*, 2012, **17**, 4811–4823.

68 F. Prati, C. Bergamini, R. Fato, O. Soukup, J. Korabecny, V. Andrisano, M. Bartolini and M. L. Bolognesi, *ChemMedChem*, 2016, **11**, 1284–1295.

69 X. Yang, P. Cai, Q. Liu, J. Wu, Y. Yin, X. Wang and L. Kong, *Bioorg. Med. Chem.*, 2018, **26**, 3191–3201.

70 J. Korabecny, R. Dolezal, P. Cabelova, A. Horova, E. Hruba, J. Ricny, L. Sedlacek, E. Nepovimova, K. Spilovska, M. Andrs, K. Musilek, V. Opletalova, V. Sepsova, D. Ripova and K. Kuca, *Eur. J. Med. Chem.*, 2014, **82**, 426–438.

71 C. Sepsova Vendula, Z. Karasova Jana, T. Gunnar, J. Daniel, J. Korabecny, et al., *Gen. Physiol. Biophys.*, 2014, **34**, 189–200.

72 A. Więckowska, M. Kołaczkowski, A. Bucki, J. Godyn, M. Marcinkowska, K. Więckowski, P. Zaręba, A. Siwek, G. Kazek, M. Głuch-Lutwin, P. Mierzejewski, P. Bieńkowski, H. Sienkiewicz-Jarosz, D. Knez, T. Wichur, S. Gobec and B. Malawska, *Eur. J. Med. Chem.*, 2016, **124**, 63–81.

73 P. N. Tripathi, P. Srivastava, P. Sharma, M. K. Tripathi, A. Seth, A. Tripathi, S. N. Rai, S. P. Singh and S. K. Shrivastava, *Bioorg. Chem.*, 2019, **85**, 82–96.

74 M. Saeedi, D. Mohtadi-Haghghi, S. S. Mirfazli, M. Mahdavi, R. Hariri, H. Lotfian, N. Edraki, A. Iraji, O. Firuzi and T. Akbarzadeh, *Chem. Biodiversity*, 2019, **16**, e1800433.

75 A. Tripathi, P. K. Choubey, P. Sharma, A. Seth, P. N. Tripathi, M. K. Tripathi, S. K. Prajapati, S. Krishnamurthy and S. K. Shrivastava, *Eur. J. Med. Chem.*, 2019, **183**, 111707.

76 M. M. Ismail, M. M. Kamel, L. W. Mohamed, S. I. Faggal and M. A. Galal, *Molecules*, 2012, **17**, 7217–7231.

77 P. K. Choubey, A. Tripathi, P. Sharma and S. K. Shrivastava, *Bioorg. Med. Chem.*, 2020, **28**, 115721.

78 T. Wichur, A. Więckowska, K. Więckowski, J. Godyn, J. Jónczyk, Á. D. R. Valdivieso, D. Panek, A. Pasieka, R. Sabaté, D. Knez, S. Gobec and B. Malawska, *Eur. J. Med. Chem.*, 2020, **187**, 111916.

